Bioorganic & Medicinal Chemistry 18 (2010) 7283–7290

Contents lists available at ScienceDirect

Bioorganic & Medicinal Chemistry

journal homepage: www.elsevier.com/locate/bmc

Intermolecular interaction and morphology investigation of drug loaded *ABA*-triblock copolymers with different hydrophilic/lipophilic ratios

Sepideh Khoee *, Hasan B. Rahimi

Polymer Chemistry Department, School of Science, University of Tehran, PO Box 14155-6455, Tehran, Iran

ARTICLE INFO

Article history:
Received 18 May 2010
Revised 2 August 2010
Accepted 4 August 2010
Available online 6 August 2010

Keywords:
ABA-triblock copolymers
Spherical morphology
Bean-like morphology
Sun-flower morphology
Nanoprecipitation
Quercetin

ABSTRACT

Copolymers with different hydrophilic/lipophilic ratios (HLR) were used to optimize the compatibility between polymer as drug carrier and quercetin as lipophilic drug. Synthesis of amphiphilic triblock copolymers (TC) of poly(butylene adipate)–poly(ethylene glycol)–poly(butylene adipate) (PBA–PEG–PBA) with different PBA molecular weights is the first approach for this purpose. Polymerization and structural features of the polymers were analyzed by different characterization techniques (GPC, ^{1}H NMR and FT-IR). Formation of hydrophobic and hydrophilic domains with different ratios in the *ABA*-triblock copolymers was studied by ^{1}H NMR. The sunflower-like nanoparticles were prepared by self-assembling of the amphiphilic copolymers in the aqueous solution. The hydrophobic PBA segments formed the central solid-like core which stabilized by the hydrophilic PEG rings. The optimum HLR for these copolymers was determined on the basis of drug release time and profile, obtained from freeze-dried nanoparticle powders. The results indicated that optimum HLR for the sustained quercetin release obtained at higher molecular weight of polyesteric domains. Zeta potential measurements showed that the nanoparticle size was close related to the initial concentrations of the nanoparticle dispersions and the compositions of the triblock copolymers. Moreover, TEM pictures showed that the nanocarriers morphologies were changed by changing HLR of triblock copolymers. The PBA–PEG–PBA nanoparticles also showed good drug loading properties, suggesting that they were very suitable as delivery devices for hydrophobic drugs.

1. Introduction

Segmented block copolymers consisting of 'hard' polyester A-blocks and 'soft' poly (ethylene oxide) [PEO] B-blocks have attracted the interest of material scientists because they allow modification of physical and chemical properties, leading to an accelerated biodegradability. These different polymers can be classified according to their structure as AB diblock, ABA or BAB triblock, multi-block, starblock and graft copolymers. BAB type triblock copolymers consisting of PEO and poly(3-hydroxybutyrate) (PHB) were investigated by coupling two chains of PEO with a low-molecular-weight isotactic PHB chain in the middle (PEO–PHB–PEO).[1] The crystallinity of PHB block in the copolymers clearly increased compared with that of the pure PHB precursor, and their critical micelle concentrations (CMCs) were in the range of 13–1100 mg/L.[2] In fact, the CMC values of the PEO–PHB–PEO copolymers were too high, especially comparing with that of poly(ε-carprolactone) (PCL)–PEG and poly(L-lactide)(PLLA)–PEG (2.5–35 mg/L).[3,4] The results implied that the PEO–PHB–PEO nanoparticles were easily dissociated upon dilution in the blood stream after intravenous injection, which was supported by the fact that all PEO–PHB–PEO copolymers were soluble in water.[2,5] The potential use of ABA-triblock copolymers as drug delivery system for hydrophilic macromolecular drugs, such as peptides and proteins was recognized in the early 1990s.[6] ABA-triblock copolymers can be designed to exhibit rapid swelling upon contact with water, forming a physically cross-linked, biodegradable hydrogel. The advantage of this approach over chemical cross-linking of PEO is the ease of incorporation of sensitive proteins and the broad spectrum of existing technologies for manufacturing such devices. Synthesis of ABA-triblock copolymers of PEO and lactic acid or glycolic acid using Sb_2O_3 and phosphoric acid as catalysts was first described by Cohn et al. in 1987.[7,8] Deng et al. used stannous chloride as catalyst to synthesize successfully ABA-triblock copolymers of PEO and PLA.[9] The application of ABA polymers for controlled release of bioactive materials emerged when shortcomings of polyesters, such as poly(lactic-co-glycolic acid) [PLGA], with respect to protein delivery became apparent and required biodegradable polymers which did not affect protein stability and release properties. Apart from these polyesters, also other biomaterials, such as poly(ortho esters) and poly(anhydrides) have been utilized. A recent review deals with various aspects of different biodegradable polymers as a platform for controlled drug delivery.[10]

* Corresponding author. Tel.: +98 2161113301; fax: +98 2166495291.
E-mail address: Khoee@Khayam.ut.ac.ir (S. Khoee).

0968-0896/$ - see front matter © 2010 Elsevier Ltd. All rights reserved.
doi:10.1016/j.bmc.2010.08.009

Currently, poly(ethylene glycol) and its derivatives have been widely used as biomedical materials. With the development of new application areas, there is a growing demand to obtain more versatile PEG derivatives. Nevertheless, an obvious disadvantage of PEG is the lack of reactive groups in the ethylene oxide units. For this reason, synthesis of PEG derivative which has reactive end groups is of great interest. In recent years, a large number of derivatives have been synthesized[11] and among them the most important PEG derivative is amino-terminated PEG.[12] However, all of these methods involved two or more synthetic steps. According to our previous studies, the BAB triblock copolymer of PEG–PBA–PEG exhibited a good carrier for a model anticancer drug. Moreover, they also showed relatively acceptable encapsulation efficiency and loading percent.[13] A considerable effort has been carried out in the last decade to relate the structure and micellar characteristics to the drug loading and release behavior from block copolymers.

In the present study, the effect of the hydrophilic/lipophilic ratio on the formation of these PEG/Polyester assemblies was examined at constant polymer concentrations. More importantly, the polymers' intermolecular interaction and morphology that are critical to the assembly of *ABA*-triblock copolymers were identified. The presence and the intensity of interactions between drug and the polymeric nanocarrier were determined by drug release profile plotting by UV spectroscopy. For this purpose, we explore the potential of the novel micelles as a drug delivery vehicle for lipophilic drugs and analyze the effects that the chemical structures of the core-forming hydrophobic block have on drug incorporation. For this purpose, we synthesized PBA–PEG–PBA triblock copolymers with three different molecular weights through condensation polymerization and using a difunctional macromonomer based on polyethylene glycol and chloro-terminated polybutyl adipate. And the polymers characterization has been studied by ^{1}H NMR, IR, DSC and GPC. To evaluate the controlled drug delivery properties of copolymer nanoparticles, quercetin, an anticancer drug was used as a model because of its very low solubility in water. Quercetin is a flavonol, plant-derived flavonoid, used as a nutritional supplement. Laboratory studies show it has anti-inflammatory and antioxidant properties, and it is being investigated for a wide range of potential health benefits. Enhancement of therapeutic efficiency of highly hydrophobic drugs may be achieved by improving their solubility. We use the PBA–PEO–PBA copolymers whose PBA blocks are longer than the PEO block, which results in very poor solubility in water. The used preparation protocol is based on the addition of dissolved PBA–PEO–PBA in acetone into an excess amount of water. We employed zetasizer and UV spectroscopy for the characterization of prepared nanoparticles.

2. Material and methods

2.1. Material

Butylene glycol, acetone and PEG (hydroxyl terminated PEG *Mw* = 2000) were purchased from Merck Chemical Co. Adipoyl chloride, tiethylamine and quercetin dihydride were obtained from Fluka Chemical Co. Diethyl ether was purchased from Guandong Guango Chemical Co. (China). All the chemicals were of analytical grade and used without any purification. PEG was vacuum-dried at 50 °C for 12 h before use.

2.2. Synthesis and characterization of triblock copolymers

2.2.1. Synthesis of end-functionalized PEG

0.098 ml (0.66 mmol) adipoyl chloride and 0.09 ml (0.66 mmol) triethylamine were added to PEG-2000 (0.66 g, 0.33 mmol) under a solvent-free condition. The reaction was carried out at 80 °C for 24 h until no more HCl released.

2.2.2. Synthesis of PBA with different molecular weights

Poly(butylene adipate) with 2000, 3000 and 4000 molecular weights were prepared by changing the feed composition according to the literature procedure[14] with some modification. The ratio between concentrations of adipoyl chloride (AC) and butylene glycol (BG) were 1:1.15 for PBA(3000)-PEG-PBA(3000); 1:1.143 for PBA(4000)-PEG-PBA(4000) and 1:1.122 for PBA(5000)-PEG-PBA(5000). A typical polymerization procedure is detailed below. 1.5 ml (10.22 mmol) adipoyl chloride and 1 mL (11.30 mmol) butylene glycol were placed in a round bottomed flask at 80 °C and 1.57 mL (11.30 mmol) triethylamine was added to the solution. Samples were removed periodically throughout the reaction in order to follow the polymerization by ^{1}H NMR and GPC. Polymerization was ended after 48 h. After that, the solution was cooled and precipitated in 50 ml of methanol to obtain crude polymers, which purified from acetone/methanol twice with 75–89% yield.

2.2.3. Synthesis of triblock copolymers with different molecular weights

Briefly, appropriate amounts of acid chloride terminated PEG were added into two equimolar of different PBA at the same temperature. The reaction was heated at 85 °C for 24 h until no more HCl was released. The viscous solution was poured into 40 ml diethyl ether and the resulting copolymers were filtered off. To separate the unreacted PEG, 80 ml H_2O was added to precipitate the copolymer and it was stirred vigorously. The white copolymer was centrifuged, decanted and purified twice more as above. The resulting copolymer was dried at a reduced temperature for 10 h.

2.2.4. Characterization of triblock copolymers

^{1}H NMR spectra of the triblock copolymers were recorded on a Bruker Avance 400 NMR spectrometer, using chloroform-d_3 ($CDCl_3$) as solvent. The composition of each copolymer was demonstrated by ^{1}H NMR. FT-IR spectra of the triblock copolymers were carried out on Shimadzu FT-IR-4300 by preparation of their potassium bromide (KBr) pellets. The number and average molecular weights of the copolymers were measured by an Agilent GPC system using tetrahydrofuran as the eluent at a flow rate of 1 ml/min at 23 °C. A calibration process was performed with polystyrene standards. Differential scanning calorimetry (DSC) thermograms of the copolymers were obtained using a computer-interfaced calorimeter (Perkin Elmer Pyres DSC) under a nitrogen atmosphere and a heating rate of 10 °C/min from ambient temperature to 350 °C. Glass transition temperature (T_g) of the copolymers was measured according to their thermograms.

2.3. Preparation and characterization of nanoparticles

2.3.1. Preparation of nanoparticles

Drug loaded nanoparticles were prepared by a nanoprecipitation method.[13] In each experiment, 10 mg of different triblock copolymers and 1.5 mg quercetin were dissolved in about 2 ml of acetone. Then the obtained organic solution was added dropwise to 10 ml distilled water under moderate stirring at room temperature. Acetone was thoroughly removed under a reduced pressure. Finally, the resulting aqueous dispersion was filtered through 0.45 μm cellulose acetate syringe filter to remove the aggregated copolymers and non-encapsulated drug crystals and then freeze-dried to extract fine nanoparticles from the aqueous medium.

2.3.2. Characterization of nanoparticle

2.3.2.1. Particle size determination. The mean diameter and size distribution of the aqueous dispersion of nanoparticles were measured by Zetasizer nano ZS (Malvern Instruments Ltd, United Kingdom). The sample was diluted to an appropriate concentration

with deionized water, which was filtered previously with a 0.45 μm Millipore filter, to avoid any contamination.

2.3.2.2. Nanoparticles yield, drug loading, encapsulation efficiency of drug loaded nanoparticles. The nanoparticles yield was obtained gravimetrically from Eq. 1. To determine the extent of drug loading and the encapsulation efficiency, an exact amount of the drug loaded nanoparticles was dissolved in 10 ml of acetone, and then the amount of quercetin in the nanoparticles was measured by ultraviolet absorption at their maximum wavelength on a Carry 100 Bio spectrophotometer. By using UV data, the drug loading content and the encapsulation efficiency were obtained from Eqs. 2 and 3, respectively. By comparing the UV spectra of pure quercetin and the quercetin loaded nanoparticles, the interactions of quercetin and polyester core of nanoparticles were also investigated:

$$\text{Nanoparticle yield}\,(\%) = \frac{\text{Weight of the nanoparticles}}{\text{Weight of the feeding polymer and drug}} \times 100 \quad (1)$$

$$\text{Drug loading content}\,(\%) = \frac{\text{Weight of the drug in nanoparticles}}{\text{Weight of the nanoparticles}} \times 100 \quad (2)$$

$$\text{Encapsulation efficiency}\,(\%) = \frac{\text{Weight of the drug in nanoparticles}}{\text{Weight of the feeding drug}} \times 100 \quad (3)$$

2.3.2.3. In vitro release of quercetin loaded nanoparticles. The in vitro release studies of quercetin from the drug loaded triblock nanoparticles were performed by the diffusion technique using a 12 kDa dialysis bag in phosphate buffer solution. This PBS solution was made of sodium hydrogen phosphate (2.83 g/l); potassium dihydrogen phosphate (0.19 g/l); and sodium chloride (8 g/l). 0.4 mg of the quercetin loaded nanoparticles and 2 ml PBS (pH 7.4) were placed into pre-swelled dialysis bag that was immersed into 100 ml PBS solution at 37 °C. Periodically, the PBS solution was withdrawn and fresh PBS was added to the release system. At measured intervals, 2 ml PBS solution was taken out and the amount of released quercetin was determined by the UV spectra. The UV spectrum for quercetin has two absorption maxima (λ_{max}) in the ultraviolet region (328 and 375 nm). The Beer–Lambert equation is:

$$A = \varepsilon c b \quad (4)$$

where A is the absorption intensity, c is the drug concentration (quercetin), b is the path length of the radiation through the absorbing medium and ε is a proportionality constant, so-called molar absorptivity. According to Beer–Lambert law, absorbance of the quercetin is directly proportional to its concentration. Therefore, by knowing the absorption intensity of the drug loaded nanoparticles (A_s) at 375 nm, the quercetin concentration (c_s) will be obtained by the following equation:

$$\frac{A_s}{A_r} = \frac{c_s}{c_r} \quad (5)$$

where, A_r and c_r are the absorption intensity and concentration of a reference sample, respectively.

2.4. Statistical analysis

In vitro release studies were performed in triplicate. The data are represented as mean ± standard deviation (SD). Data were analyzed using the Student t test. Statistical significance was set at $P < 0.05$.

3. Results and discussion

3.1. Synthesis and characterization of the copolymers

ABA-triblock copolymers with different lengths of PBA were synthesized via a three-step reaction (Scheme 1). Firstly, a dihydroxyl terminated PEG was end-functionalized using adipoyl chloride. At the second step, hydroxyl terminated PBAs with different molecular weights were synthesised according to Table 1. The resulting polymers were reacted with PEG, obtained from the first step to produce triblock copolymers with a central core of PEG and different lengths of PBA as terminal blocks. Each polymerization was sampled at different time intervals and analyzed by ^{1}H NMR and GPC for measurement of conversion, molecular weight and polydispersity.

The structure of triblock copolymers were characterized by ^{1}H NMR. In $CDCl_3$, where micellar formation was not expected, all ^{1}H NMR resonances attributed to PBA and PEG units were detected. Presence of methylene protons of PEG and PBA blocks showed successful formation of the triblock copolymer. Assignment of methylene protons adjacent to the carbonyl groups of the adipic segments at 2.35 ppm, methylene protons adjacent to the hydroxyl groups of the butylene glycol segments at 4.09 ppm and remained methylene protons of the butylene glycol and adipic acid units at 1.67 ppm for the PBA blocks have been shown in Figure 1. Methylenic protons of PEG at 3.95 ppm were also observed in ^{1}H NMR spectrum.

The results showed that PBA–PEG–PBA block copolymers of *ABA* type were mainly formed. The absence of a sharp signal at

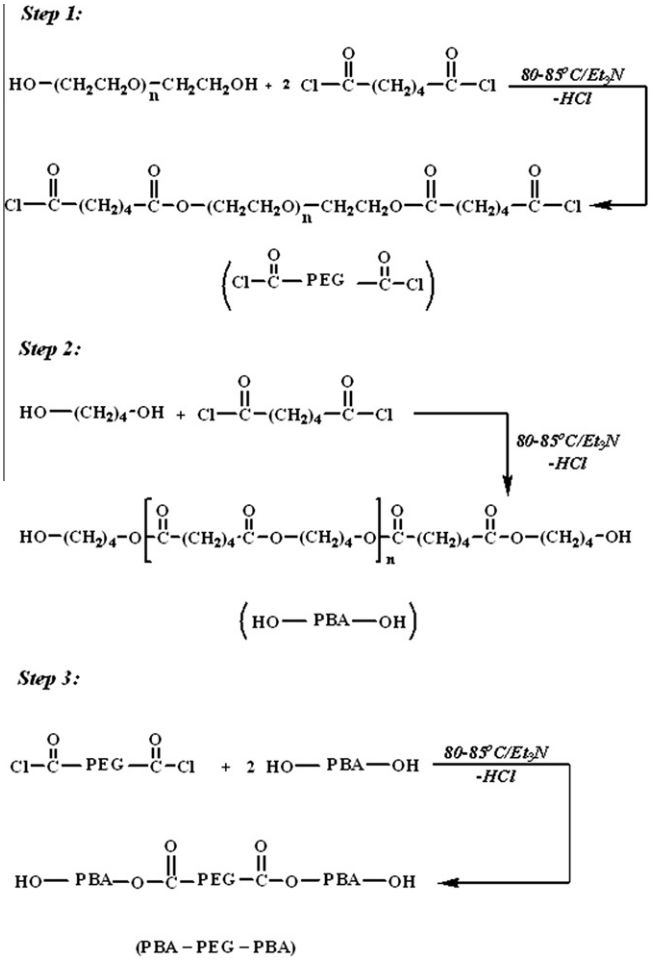

Scheme 1. Synthesis of the triblock copolymers based on PBA and PEG.

Table 1
Polymerization condition for preparation of different molecular weights of PBA–PEG–PBA

Sample	AC/BG[a]	AC/BG[b]	PBA[b] (g/mol)	PEG (g/mol)	Yield (%)
PBA-3000	1:1.150	1:1.211	2090	2000	71
PBA-4000	1:1.143	1:1.182	2397	2000	84
PBA-5000	1:1.122	1:1.107	3914	2000	89

[a] Molar fraction of adipoyl chloride to butylene glycol in the feed to produce 3000, 4000 and 5000 molecular weights of PBA.
[b] Obtained from ^{1}H NMR.

Table 2
Molecular weight characteristics of different triblock copolymers

Sample	Mn[a]	Mn[b]	Mw[b]	Mw/Mn[b]
TC-8000	6180	3304	6136	1.86
TC-10000	6794	4735	8105	1.71
TC-12000	9828	6393	10,107	1.58

[a] Obtained PBA–PEG–PBA molecular weights from ^{1}H NMR.
[b] Obtained PBA–PEG–PBA molecular weights from GPC.

2.63 ppm in their ^{1}H NMR spectra due to the terminal OH group in the PEG moiety rejected the coexistence of PBA–PEG copolymer of *AB* type. Calculations were performed by ^{1}H NMR due to the comparison of relative integration of the signals at 3.67 ppm assigned to the protons of PEG and that at 4.12 ppm for methylene protons of PBA. The mean molecular weights of PBA portions and block copolymers were calculated as bellow and have been listed in Table 1:

$$A_{3.67}/[M_{PEG}/44] = A_{4.12}/[2(M_{PBA}/200)]$$

$$M_{PBA} = 4545.45(A_{4.12}/A_{3.67})$$

where M_{PEG} and M_{PBA} are the mean molecular weights of PEG and PBA blocks in the copolymer, respectively; $A_{3.67}$ and $A_{3.67}$ are the peak areas at 3.67 ppm and 4.12 ppm in ^{1}H NMR, respectively; 44 and 200 are the molecular weights of $-CH_2CH_2O-$ and $-CO(CH_2)_4CO-O(CH_2)_4O-$ units, respectively in the block copolymers. The feeding molar ratios of AC to BG were chosen to be 1:1.150, 1:1.143 and 1:1.122 at which the hydrophobic parts of the copolymer would have molecular weight of 3000, 4000 and 5000 g/mol. However, the actual AC/BG ratios in the copolymers, which were determined by ^{1}H NMR spectra, deviates a little from the theoretical feeding ratios and possibly due to the partial copolymerization and removal of oligomers during purification process.

The molecular weights and molecular weight distributions of these block copolymers were determined by GPC too. From Table 2, it was found that the Mw of block copolymers obtained from GPC were in good agreement with those obtained from ^{1}H NMR. On the other hand, the single peak in the GPC chromatograms of the products indicated that the products had a unique structure.

Moreover, FT-IR results of different triblock copolymers have been shown in Figure 2. PBA–PEG–PBA block copolymers presented distinct carbonyl stretching band at 1710 cm^{-1} and the characteristic C–O bonds at 1261 cm^{-1} for the esteric groups within PBA block, the broad C–O–C band at 1170 cm^{-1} and C–H peaks at 2850 cm^{-1} assignable to the etheric linkages of PEG block. Meanwhile, the relative intensities of carbonyl bands within PBA blocks to the C–H stretching bands within PEG block increased gradually with the increasing block length of PBA.

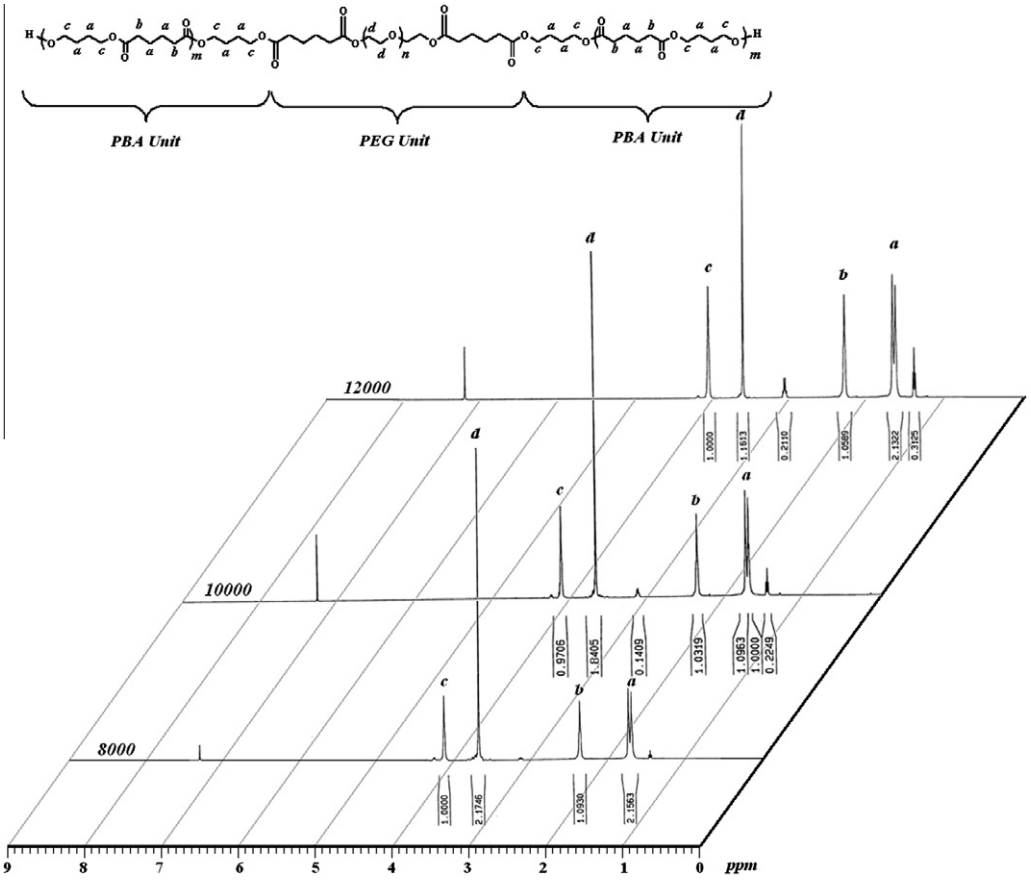

Figure 1. ^{1}H NMR of the triblock copolymers (a) TC-6000, (b) TC-8000 and (c) TC-10000.

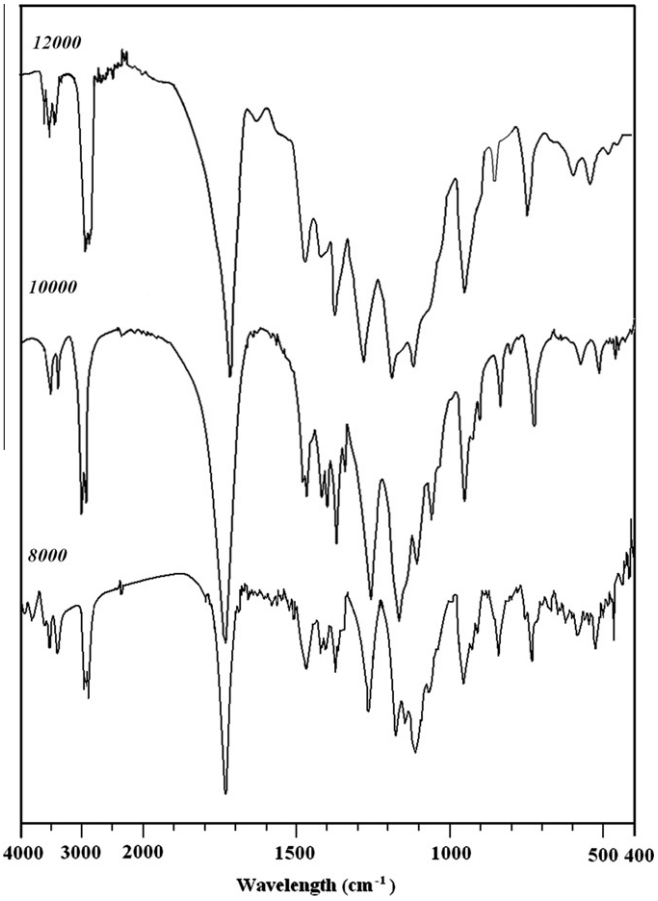

Figure 2. FT-IR of the triblock copolymers (a) TC-8000, (b) TC-10000 and (c) TC-12000.

We used differential scanning calorimetry (DSC) to investigate thermal properties of PBA–PEO–PBA triblock copolymers (Fig 3). With respect to the melting points of PEG (50.8 °C) and PBA (60.6 °C) homopolymers, these block copolymers showed different thermal behaviors. The block copolymer consisting PBA(3000)-PEG(2000)-PBA(3000) and PBA(4000)-PEG(2000)-PBA(4000) exhibited melting endotherms at 54.6 and 59.7 °C, respectively.

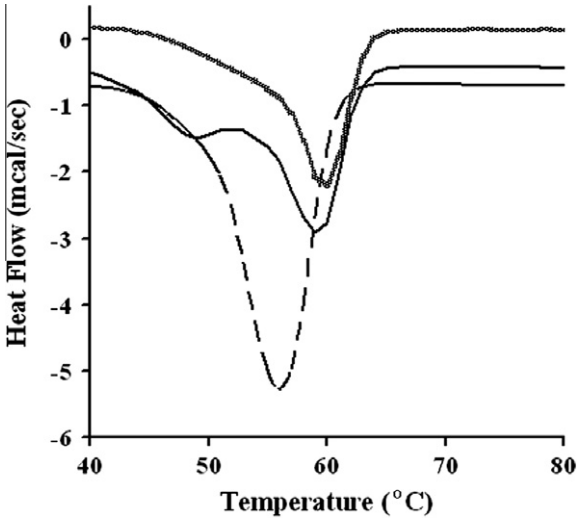

Figure 3. DSC thermograms of PBA–PEG–PBA triblock copolymers: TC-12000 (—), TC-10000 (○○○○) and TC-8000 (– – –).

An intermediate melting point compared with their parent homopolymers, indicated phase compatibility and in agreement with those mentioned in the literature.[15,16] For longer PBA chains (TC-12000), no overlapped melting endotherm was found. This might be due to a decrease in compatibility of the shorter PEG chain with dominant PBA blocks and sufficient phase separation. In fact, the DSC analysis of PBA–PEG–PBA copolymers showed that the PEG blocks have greatly hampered the crystallization of PBA blocks and the degree of crystallinity of PBA blocks (within copolymers) decreased with the decreasing block length of PBA. In comparing to our previous work,[13] it could be seen that *BAB* type TCs with long polyester segments were essentially produced semicrystalline polymers with two Tgs due to the phase separation. Whereas, dividing of the long polyester segments into two equal parts in *ABA* type triblocks (at constant lipophilic to hydrophilic ratio) produces monophasic matrix with an average lower T_g with respect to its parent homopolymers. This decrease in T_g in the *ABA*-triblock copolymers indicated a better phase compatibility compared with the *BAB* ones with similar HLB.

3.2. Synthesis and characterization of the nanoparticles

Core-shell type nanoparticles of PBA–PEG–PBA triblock copolymers were prepared by the nanoprecipitation method widely employed to produce nanoparticles by interfacial deposition of a polymer followed by displacement of an organic polar solvent in water. Nanoprecipitation was carried out without addition of any surfactant in the water phase to highlight the surfactant-like properties of the copolymers. Size and size distribution of the nanoparticles were measured by zetasizer and the mean diameter of polymer nanoparticles was in the range of 123–183 nm (Fig. 4). Particle sizes decreased with the increasing in the length of incorporated PBA block into the copolymer chains. Amphiphilic copolymers with shorter hydrophobic PBA block are more hydrophilic, and they can diffuse more easily into the aqueous medium. So because of the aggregation of nanoparticles after redispersion, they could accumulate and result in larger nanoparticles (Fig. 4c). When the copolymer chain has long PBA blocks, more hydrophobic copolymers layer will be obtained which could pack the PBA domain in the core of flower-like micelle and so, more hydrophobic nanoparticles will be formed easily (Fig. 5). Furthermore, it could be seen that nanoparticles with PBA 5000 and 4000 show a unimodal size distribution (Fig. 4a and b), while nanoparticles with PBA 3000 have a trimodal size distribution. The observed trend shows that by decreasing the polyester molecular weight, the aggregation tendency for the formation of large clusters is increased. Appearance of a new peak at 5190 nm and its accretion with time proves the above hypothesis (Fig. 4c).

To examine the aggregation amount of nanoparticle solutions, we determined the particle size of produced nanoparticles by changing the copolymer concentration (Table 3). For all triblock copolymers with different molecular weights, the particle size decreased with the decrease in solution concentration. In this situation, nanoparticles could be only produced separately and no trace of cluster was observed (Scheme 2). For a concentration of 0.4 mg/mL of nanoparticles, the particle size was slightly decreased for PBA 5000 and 4000. More significant particle size decreasing was observed for PBA 3000 (Fig 4d), which implies that decreasing the nanoparticle concentration leads to a decrease in the carriers' particles size.

TEM measurement was carried out to characterize the morphology of PBA–PEG–PBA nanoparticles. Figure 5 shows the images of copolymer TC-12000 and TC-8000 nanoparticles. When two hydrophobic PBA blocks were attached to the PEG chain, the polymer was triggered to self-assemble in water. In TC-8000 and TC-10000, most of the nanoparticles were observed to have a spherical

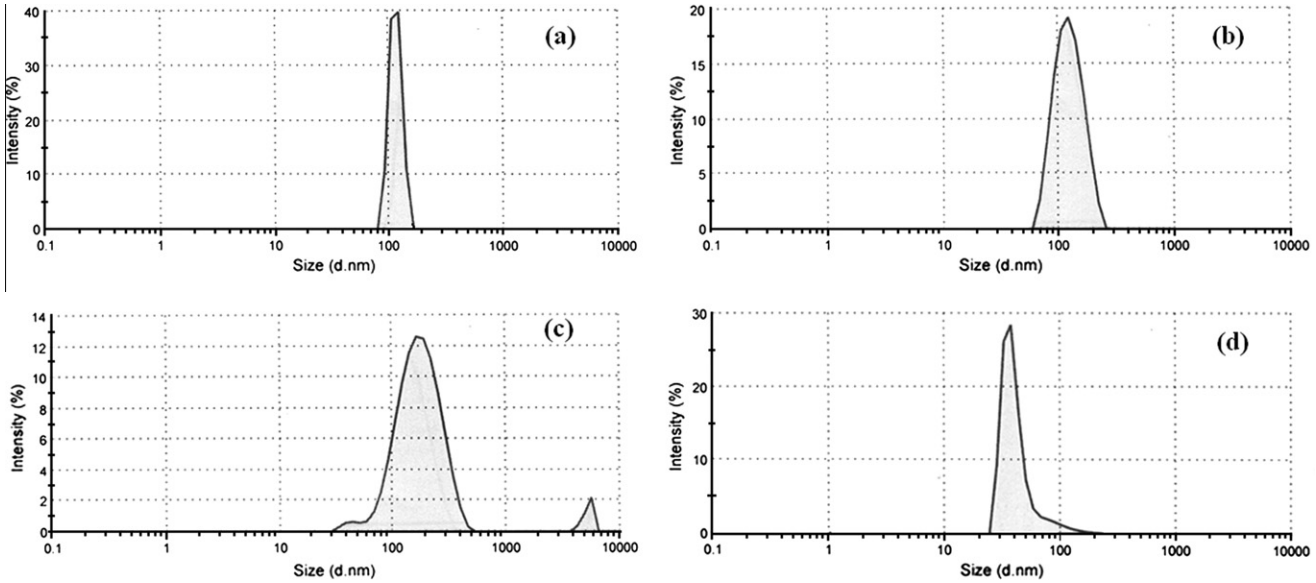

Figure 4. Size distributions for different triblock copolymers at 1 mg/ml triblock concentration: (a) TC-12000; (b) TC-10000; (c) TC-8000 and at 0.4 mg/ml triblock concentration: (d) TC-8000.

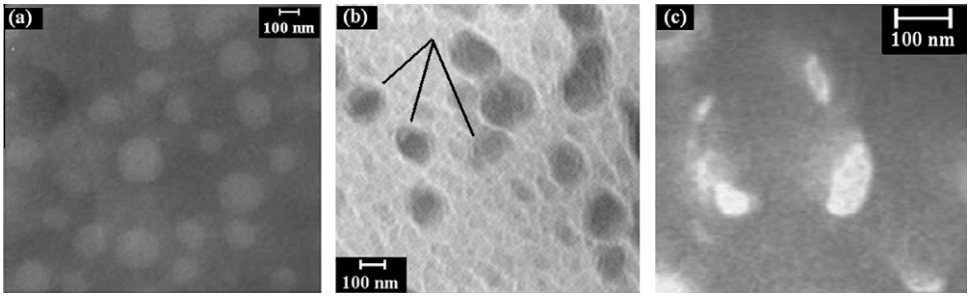

Figure 5. TEM pictures of TC-8000 (a) and TC-12000 (b and c) nanoparticles.

Table 3
Particle size and polydispersity index of drug loaded triblock copolymers at different concentration of nanoparticles

Sample	Particle size[a] (nm)	PDI[a]	Particle size[b] (nm)	PDI[b]
TC-8000	183 ± 7.9	0.44	43.8 ± 2.3	0.12
TC-10000	126 ± 5.7	0.30	67.3 ± 4.0	0.26
TC-12000	115 ± 6.1	0.07	85.2 ± 8.6	0.23

[a] Calculated at 10 mg of nanoparticles in 10 ml of water.
[b] Calculated at 10 mg of nanoparticles in 25 ml of water.

shape, and the average sizes of the nanoparticles were in the range of 126–183 nm. Whereas, the morphology changed from spherical to bean-like by increasing the PBA block length to 12,000 (Fig. 5b and c). This change from spherical shape to cylindrical shape can be expected only if the soluble block of the copolymer is shorter than the insoluble blocks of that.[17] It seems that the present morphology is a result of thermodynamic equilibrium during self-assembling process, while the micelles are being formed in acetone/water mixture. The thermodynamic of self-assembling depends on three parameters during the formation of block copolymer micelles: (i) core formation, (ii) corona–solvent interaction and (iii) core–solvent interaction. The contribution of core formation, which is influenced by several factors, may be the most important parameter. The polyester chains in the spherical core are stretched in the radial direction. Therefore, it is of interest that the stretching decreases as the shape changes from spherical to bean-like morphology; especially by increasing the hydrophobic portions at constant hydrophilic one.

Encapsulation efficiency (EE), drug loading and release features of nanoparticles were calculated from the absorbance measurement of quercetin at 370 nm by UV spectrophotometer. There is no interference by the copolymers at this wavelength. These properties of quercetin loaded nanoparticles prepared at two different concentrations have been reported in Table 4. Drug loading content and EE depend on the composition of copolymers and arrangement of the micelles. For both concentrations, drug-loading and EE increased with the increase in the molecular weight of PBA blocks. This can be reasonably attributed to the fact that the extent of polymer/drug hydrophobic interactions increases with the increasing block length of PBA. It was found that the decrease in concentration of the copolymers did not affect on the EE values, while the drug loading increased except for TC-12000 nanoparticles. TEM picture of TC-8000 at high concentration (Fig. 6a) displays the presence of some aggregated samples with thin shell, meaning that some of the hydrophobic parts of the copolymer act as a linker instead of being just as a shell layer. Whereas, all nanoparticles will appear separately in the samples at low concentration of copolymers (Fig. 6b). This causes producing particles with thicker shell and consequently, releasing of the drug will be decreased dramatically during nanoparticles preparation and freeze drying time interval. The particle size of TC-12000 in high and low concentrations does not vary as high as TC-8000, depicting that their charac-

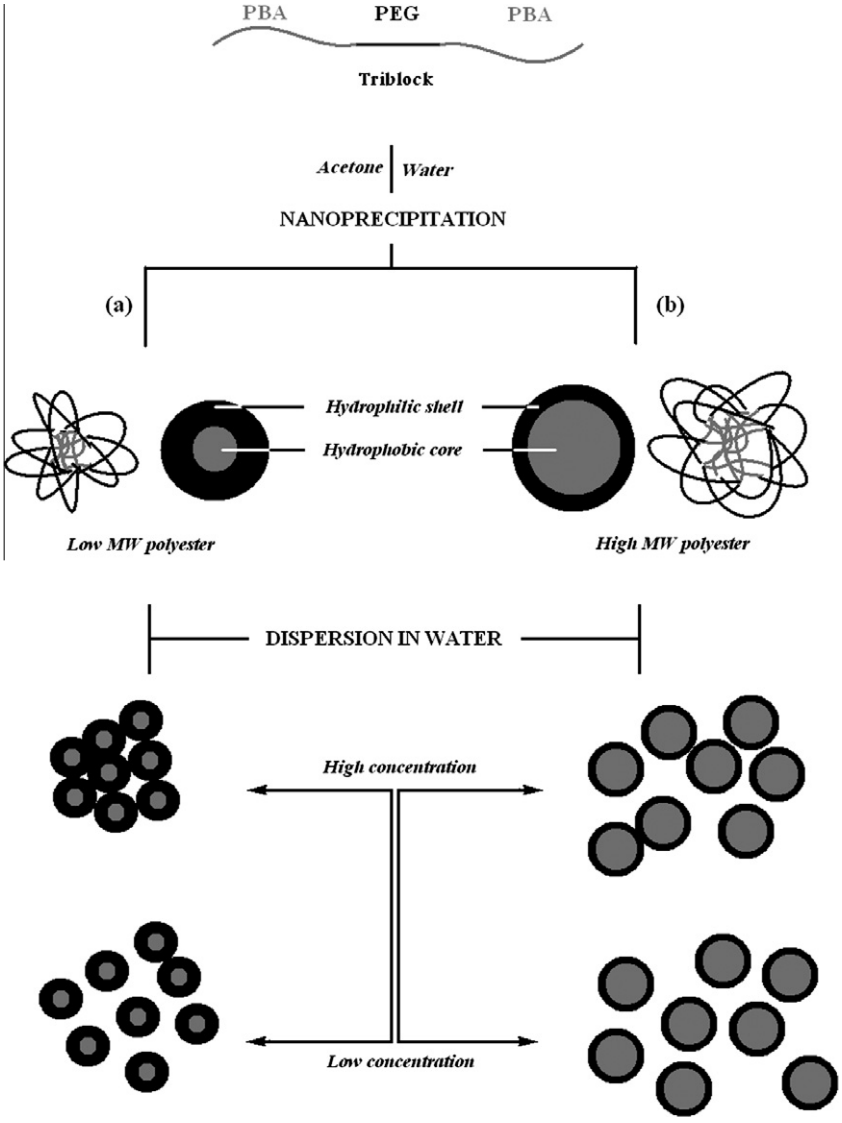

Scheme 2. Schematic representation of variation in particle size at different nanoparticles concentration solutions prepared from low (a) and high (b) molecular weight polyesters.

Table 4
Drug loading and encapsulation efficiency of the obtained quercetin loaded nanoparticles for different triblock copolymers at two concentrations

Sample	Drug loading[a] (%)	EE[a] (%)	Drug loading[b] (%)	EE[b] (%)
TC-8000	2.6	5.3 ± 1.0	3.84	4.86 ± 0.2
TC-10000	8.45	29 ± 1.4	8.62	27.9 ± 2.2
TC-12000	11	51 ± 2.7	10.97	49.35 ± 3.8

[a] Calculated at 10 mg of nanoparticles in 10 ml of water.
[b] Calculated at 10 mg of nanoparticles in 25 ml of water.

teristics that is, EE and drug-loading must not be affected by changing the concentration.

Therefore, the increase in drug loading and encapsulation efficiency for quercetin loaded nanoparticles can be assumed to be mainly dependent on the drug incorporation into the nanoparticles. This hypothesis is further supported by the fact that the compatibility of drug and hydrophobic core of nanoparticles is a determining factor.[18] It was clearly demonstrated that by increasing the number of interactions between quercetin and the polyesters from TC-8000 to TC-10000 and TC-12000, the drug-loading in the nanoparticles rose considerably from 2.6% to 8.45% and finally to 11%, respectively. As a result, a higher density of the esteric functional groups in the polyesteric segments (more polarity and boosted affinity) causes more hydrogenic interactions between the hydroxyl groups of quercetin and the esteric functional groups of the polyesters in the triblock copolymers. Hence, the drug–polymer affinity and drug-loading content were improved significantly.

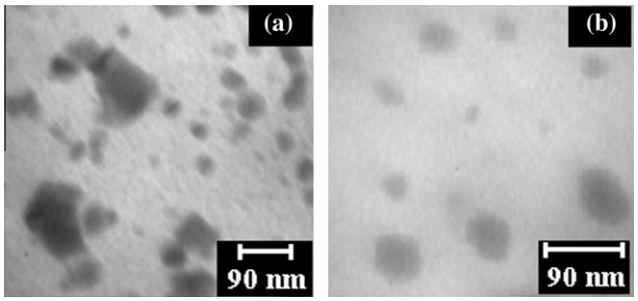

Figure 6. TEM pictures of TC-8000 with 10 mg/10 ml (a) and 10 mg/25 ml concentrations (b).

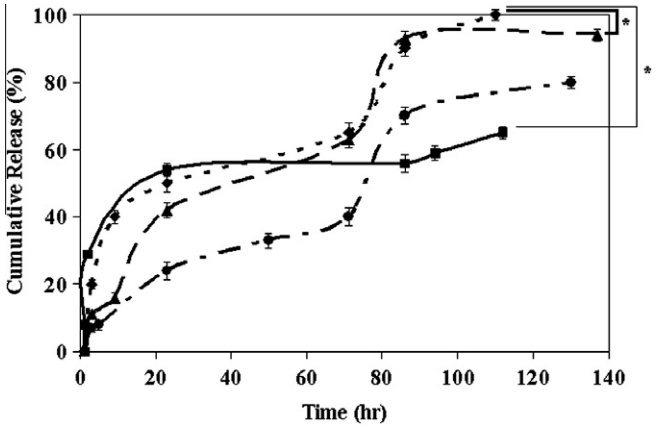

Figure 7. In vitro release profiles of different triblock copolymers at 1 mg/ml triblock concentration for: TC-12000 (— — —); TC-10000 (– – – –); TC-8000 (– – –) and at 0.4 mg/ml triblock concentration for: TC-8000 (—). The results represent the means ± SEs ($n = 3$). The asterisks (*) indicate statistical significance ($p < 0.05$).

In vitro release behavior of quercetin was studied in PBS (0.1 M, pH 7.4) at 37 °C. The free quercetin completely released during 1 day, while the drug in micelles released as long as 150 h and more (Fig. 7). It can be seen that the release profile of quercetin from the *BAB* triblock copolymer with 2:5 of hydrophilic to hydrophobic ratio, revealed an initial burst release up to 54 ± 3.4% and then a slow release profile was observed. On the other hand, the release profile of *ABA*-triblock copolymer is quite different. Higher burst release was found with formulations containing shorter PBA block lengths. We found 50.0 ± 2.1%, 40 ± 4.0%, and 24 ± 2.6% burst release of quercetin from formulations containing PBA 3000, 4000 and 5000, respectively. Higher molecular weight of polymer causes a decrease in the burst release. The release profile of quercetin from the ABA type copolymers presents three phases: an initial burst release phase in which 24–50% of the entrapped drug was released during 24 h, a plateau region in which a limited amount of drug was released during 72 h, and a sequential high release phase in which 75–93% of the drug was released in a continuous way. Compared to the large burst release of quercetin from *BAB* copolymers (54 ± 4.1%), this copolymer can decrease burst release to a relatively low level. The phenomenon is usually due to the presence of surface deposition of drug and sequential drug release may be according to the diffusion of drug from the polymeric shell as well as due to erosion of polymer. This typical system is thought to have a core-shell structure in an aqueous environment. It has a flower-type micellar shape, in which the middle hydrophilic PEG chain forms a sphere around the surface and hydrophobic PBA resides in the core. Generally, the drug release rate from nanoparticles with low-molecular-weight is relatively faster than that with the higher ones. In these systems, hydrophobic cores that are composed of polyester segments have good inclusion capacity of hydrophobic drugs. Short hydrophobic PBA blocks in the core, follows a limited interaction between the drug and PBA. More works are necessary to determine that this remarkable decrease in the burst release in TC-12000 is due to the increase in MW or change in the morphology. However, both of these variations can result in a good compatibility and interaction between quercetin and hydrophobic domain of ABA copolymers, which cause to prolong the presence of drug in the core of nanoparticles.

4. Conclusions

The current research demonstrates that small variations in the hydrophilic/lipophilic ratio of copolymers can lead to significant differences in their intermolecular interactions (affecting on size) and morphology of nanocarriers. Drug loaded nanoparticles can be effectively obtained by nanoprecipitation of triblock copolymers to produce nanocarriers of 115–183 nm in size. Interestingly, at high TC concentration, those TCs with lower HLR produce smaller nanoparticles even at higher molecular weight. The low concentration of triblock copolymers self-assemble in the aqueous media with mean size in the range of 43–85 nm and at this condition, the smallest nanoparticles come from the higher HLR. Nanoparticles prepared from TC dispersions exist in two morphologies including spherical and cylindrical shapes. TEM studies proved that the structure of nanoparticles in the solution depended on their initial polymer molecular weights. The morphology variety of TCs was dependent on the chain length of the PBA blocks. The presence of nanoparticles with spherical and cylindrical morphologies would allow us to investigate the morphological effect on the drug release efficiency. At high HLR, a weak interaction between polymer and drug was resulted in the formation of nanoparticles with low percent of drug loading and encapsulation efficiency and high percent of burst release. Constant PEG length at the center of copolymer chains and long PBA blocks at either ends (low HLR) increase the encapsulation efficiency and drug loading, while decreases the burst release of quercetin as a hydrophobic drug. Thus, structural tailoring of functional multi-block copolymers via condensation polymerization provides a unique and versatile condition to produce different carriers for drug delivery.

Acknowledgments

We thank Dr. Mahdavian and his group at Iran Polymer and Petrochemical Institute (IPPI), Tehran, for recording GPC analysis. Also helpful assistance of Mr. Hashemi for taking TEM micrographs from Faculty of Science, University of Tehran is greatly acknowledged.

References and notes

1. Li, J.; Li, X.; Ni, X. P.; Leong, K. W. *Macromolecules* **2003**, *36*, 2661.
2. Li, J.; Li, X.; Ni, X. P.; Tan, N. K. *Langmuir* **2005**, *21*, 8681.
3. Yasugi, K.; Nagasaki, Y.; Kato, M.; Kataoka, K. *J. Controlled Release* **1999**, *62*, 89.
4. Hagan, S. A.; Coombes, A. G. A.; Garnett, M. C.; Dunn, S. E.; Davies, M. C.; Illum, L.; Davis, S. S. *Langmuir* **1996**, *12*, 2153.
5. Chen, C.; Yu, C. H.; Cheng, Y. C.; Yu, P. H. F.; Cheung, M. K. *Eur. Polym. J.* **2006**, *42*, 2211.
6. Youxin, L.; Volland, C.; Kissel, T. *J. Controlled Release* **1994**, *32*, 121.
7. Younes, H.; Cohn, D. *J. Biomed. Mater. Res.* **1987**, *21*, 1301.
8. Cohn, D.; Marom, G.; Younes, H. Design and Synthesis of Biodegradable Poly(ether-esters). In *Biomaterials and Clinical Applications*; Pizzoferrato, A., Marchetti, P. G., Ravaglioli, A., Lee, A. J. C., Eds.; Elsevier Science B.V.: Amsterdam, 1987; pp 503–510.
9. Deng, X. M.; Xiong, C. D.; Cheng, L. M.; Xu, R. P. *J. Polym. Sci., Polym. Lett. Ed.* **1990**, *28*, 411.
10. Kissel, T.; Li, Y.; Unger, F. *Adv. Drug Delivery Rev.* **2002**, *54*, 99–134.
11. Khoee, S. Preparation of Nanostructured Polymeric Particles for Drug Delivery Applications and the Affecting Parameters. In *Advances in Nanotechnology*; Chen, E. J., Peng, N., Eds.; Nova Science Publishers.: New York, 2010; Vol. 1,.
12. Tian, W.; Chen, Q.; Yu, C.; Shen, J. *Eur. Polym. J.* **2003**, *39*, 1935.
13. Khoee, S.; Hassanzadeh, S.; Goliaie, B. *Nanotechnology* **2007**, *18*, 175602.
14. Khoee, S.; Yaghoobian, M. *Eur. J. Med. Chem.* **2009**, *44*, 2392–2399.
15. Lu, F. Z.; Meng, J. Q.; Du, F. S.; Li, Z. C.; Zhang, B. Y. *Macromol. Chem. Phys.* **2005**, *206*, 513.
16. You, L. C.; Lu, F. Z.; Li, Z. C.; Zhang, W.; Li, F. M. *Macromolecules* **2003**, *36*, 1.
17. Zhang, L.; Eisenberg, A. *Science* **1995**, *268*, 1728–1731.
18. Kumar, V.; Prud'Homme, R. K. *J. Pharm. Sci.* **2008**, *21342*, 1.